Interactions of C. frondosa-derived inhibitory peptides against angiotensin I-converting enzyme (ACE), α-amylase and lipase

Yi Zhang, Shudong He, Xin Rui, Benjamin Simpson

Interactions of *C. frondosa*-derived inhibitory peptides against angiotensin I-converting enzyme (ACE), α-amylase and lipase

Yi Zhang [1,2 *], Shudong He [3], Xin Rui [4], Benjamin K. Simpson [1, *]

[1] Department of Food Science and Agricultural Chemistry, McGill University, Ste-Anne-de-Bellevue, Québec, Canada H9X 3V9

[2] IPREM, E2S UPPA, CNRS, Université de Pau et des Pays de l'Adour, 64000 Pau, France

[3] School of Food and Biological Engineering, Hefei University of Technology, Hefei 230009, Anhui, China

[4] College of Food Science and Technology, Nanjing Agricultural University, Jiangsu Province, China

* Corresponding author:

Dr. Benjamin K. Simpson

Tel: +1 514-398-7737; E-mail: benjamin.simpson@mcgill.ca

First author & co-corresponding author:

Dr. Yi Zhang; E-mail: yi.zhang10@mcgill.ca

Other authors:

Dr. Shudong He. E-mail: shudong.he@hfut.edu.cn

Dr. Xin Rui. E-mail: ruix@njau.edu.cn

Abstract

The study illustrates the molecular mechanisms by which marine-derived peptides exhibited different structures and inhibition functions to concurrently inhibit multiple enzymes involved in chronic diseases. Peptides (2 mg/mL) exhibited inhibition against angiotensin-converting enzyme (ACE, inhibition of 52.2−78.8%), pancreatic α-amylase (16.3−27.2%) and lipase (5.3−17.0%). Further in silico analyses on physiochemistry, bioactivity, safety and interaction energy with target enzymes indicated that one peptide could inhibit multiple enzymes. Peptide FENLLEELK potent in inhibiting both ACE and α-amylase showed different mechanisms: it had ordered extended structure in ACE active pocket with conventional H-bond towards Arg_{522} which is the ligand for activator Cl^-, while the peptide folded into compact "lariat" conformation within α-amylase active site and the K residue in peptide formed intensive H-bonds and electrostatic interactions with catalytic triad Asp_{197}−Asp_{300}−Glu_{233}. Another peptide APFPLR showed different poses in inhibiting ACE, α-amylase and lipase, and it formed direct interactions to lipase catalytic residues Phe_{77} & His_{263}.

Keywords

Peptides; inhibition; ACE; α-amylase; lipase

1. Introduction

Peptides produced from foods can perform inhibitory activities against enzymes involved in chronic diseases. Although synthetic inhibitor compounds are mainly used to combat chronic diseases, their negative side effects such as hepatotoxicity, necessitate the discovery of natural bioactive peptides as alternatives (Daliri, Lee, & Oh, 2018). Angiotensin I-converting enzyme (ACE, EC 3.4.15.1) plays a key role in the regulation of blood pressure via renin-angiotensin system and kallikrein-kinin system by means of converting inactive decapeptide angiotensin-I into potent vasoconstrictor angiotensin-II, as well as inactivating the vasodilator bradykinin (Toopcham, Mes, Wichers, Roytrakul, & Yongsawatdigul, 2017). Pancreatic α-amylase (EC 3.2.1.1) catalyzes the hydrolysis of α-linked polysaccharides (e.g., starch) for glucose production, and its inhibition results in a reduction of blood glucose levels after carbohydrate diet for controlling type 2 diabetes (Admassu, Gasmalla, Yang, & Zhao, 2018). Lipase (EC 3.1.1.3) acts specifically on the ester bonds of triglycerides to release free fatty acids, mono- and di- glyceride, and its inhibitors, e.g., a commercialized drug “orlistat”, can delay the absorption of free fatty acids into systemic circulation and adipocytes (Rajan, Palaniswamy, & Mohankumar, 2020) for obesity management. Moreover, hypertension, diabetes and obesity are correlated, and unhealthy diet is one of their fundamental causes. Thus, it is of great interest to discover and understand the mechanisms of food-derived peptides with inhibitory activity against enzymes such as these.

The source of the peptides in this research is a marine species, Atlantic sea cucumber (*Cucumaria frondosa*). Our previous study disclosed antioxidant peptides from *C. frondosa* via enzymatic hydrolysis (Zhang, He, Bonneil, & Simpson, 2020b) similar to antioxidant peptides from foods such as rice bran and beans (Ngoh & Gan, 2016; Wang, Chen, Fu, Li, & Wei, 2017), and these peptides with multi-functions have potential research and application value. Currently,

in silico approaches based on peptide database and computational programs are widely used in combination with conventional *in vitro*/*in vivo* methods to study bioactive peptides in terms of screening, proteolysis, bioactivity, toxicity and allergenicity, and to derive information on their binding conformations and interactions with enzymes (Kang, Jin, Lee, Kim, Koh, & Lee, 2020; Zhang, Aryee, & Simpson, 2020a). In this study, peptides with inhibitory activities against ACE, pancreatic α-amylase, and pancreatic lipase were obtained *in vitro*, and the identified peptide sequences were analyzed using *in silico* tools to assess their properties and interpret inhibition mechanisms.

2. Materials and methods

2.1. Enzymes, chemicals, and peptides

ACE (from rabbit lung), α-amylase (from porcine pancreas), lipase (Type II, from porcine pancreas), and chemicals including acetonitrile (ACN), 3,5-dinitrosalicylic acid (DNS), ethyl acetate, formic acid, Hip-His-Leu, maltose, olive oil, phenolphthalein, starch, and triton X-100 were purchased from Sigma-Aldrich Co., USA. Peptides were produced from fresh *C. frondosa* using alcalase (A) and trypsin (T) with concentrations of 3000 and 2000 U/g at a ratio of 1:3 (w/v), respectively. The reaction mixture was incubated with agitation at 25 °C for 2 h; afterwards, the mixture was heated at 100 °C for 1 min to inactivate enzymes, and further filtered with 0.22 μm membranes (Millipore, USA). Peptides were fractioned using 10 kDa, 5 kDa, 3 kDa and 2 kDa cut-off ultrafiltration membranes (Millipore, USA) centrifuged at 3000 g, and 14 peptide fractions ($A_{<10}$, $A_{10–5}$, $A_{<5}$, $A_{5–3}$, $A_{<3}$, $A_{3–2}$, $A_{<2}$, and $T_{<10}$, $T_{10–5}$, $T_{<5}$, $T_{5–3}$, $T_{<3}$, $T_{3–2}$, $T_{<2}$) were obtained. The peptides in $A_{<2}$ and $T_{<2}$ fractions were subsequently selected based on their relatively high multi-enzymes inhibitory properties and identified using LC-MS/MS and Peaks

88 software (Zhang et al., 2020b).

89 **2.2. Determinations of multi-enzyme inhibitory activities**

90 ACE inhibitory activity of peptides was determined based on the method described
91 previously (Zhang, Li, Fu, & Mou, 2019) with Hip-His-Leu as substrate to produce hippuric acid
92 at 37 ^{o}C, pH 8.3, and the reaction was terminated by HCl and measured spectrophotometrically
93 at 280 nm. Alpha-amylase inhibitory activity of the peptides was determined using starch as
94 substrate to produce maltose at 37 ^{o}C, pH 6.0, and the reaction was terminated by adding the
95 color reagent containing DNS, potassium sodium tartrate and NaOH then measured
96 spectrophotometrically at 540 nm (Cardullo et al., 2020). The amount of generated maltose was
97 calculated using a standard curve (0–0.2%, w/v). Lipase inhibitory activity of peptides was
98 determined using olive oil as substrate to produce free fatty acids at 37 ^{o}C, pH 7.5. The assay
99 was terminated by boiling the reaction mixture before measuring fatty acids by titration with
100 NaOH using phenolphthalein as indicator (Huang, Chow, & Tsai, 2012).

101 **2.3. Characterizations of peptide biochemical properties**

102 Peptide sequences were submitted to various *in silico* tools listed in **Table S1**.
103 Physiochemical properties including isoelectric point (pI), water solubility and hydrophobicity of
104 the peptides were predicted using Peptide property calculator. Probability of bioactivity was
105 predicted using PeptideRanker (Han, Maycock, Murray, & Boesch, 2019). Inhibitory activities
106 towards ACE, α-amylase and lipase were predicted by BIOPEP-UWM using "Bioactive peptides"
107 database and "Analysis" program. Location of bioactive fragments in a peptide and the
108 frequency of bioactive fragments occurrence (parameter A) were returned (Minkiewicz, Iwaniak,
109 & Darewicz, 2019). Toxicity was predicted using ToxinPred where SVM-based method with
110 threshold value of 0.0 was selected (Gupta et al., 2013). Allergenicity was predicted using

111 "Allergenic proteins with their epitopes" database in BIOPEP-UWM.

112 **2.4. Molecular docking**

113 Molecular docking between each peptide and enzymes ACE, α-amylase and lipase,
114 respectively, was performed using BIOVIA Discovery Studio (Accelrys, San Diego, CA, USA).
115 The crystal structures of human ACE (PDB ID: 1O8A), human pancreatic α-amylase (PDB ID:
116 5KEZ) and human pancreatic lipase (PDB ID: 1LPB) were obtained from Protein Data Bank
117 (PDB). The enzyme structures were optimized to minimize the energy and to remove water
118 molecules before docking. CDOCKER docking program was applied where a more negative
119 CDOCKER energy, i.e., higher (−)CDOCKER energy value, indicated more favorable docking
120 affinity, and "F" means docking failure (Zhang et al., 2020b). The binding site of each enzyme
121 contained its active site, and the values of binding site were adjusted according to those reported
122 for enzyme – reference peptide interaction as follows: binding sites for ACE were created using
123 the coordinates x: 36.189, y: 43.643, z: 55.175 and a radius of 16 Å. A known ACE inhibitory
124 peptide, PRY (Fu, Alashi, Young, Therkildsen, & Aluko, 2017) was used as control (C1). The
125 docking of α-amylase was carried out with a radius of 16 Å and coordinates x: -5.95348, y:
126 3.30228, z: -25.4401. A known α-amylase peptide, YPYSCWVRH (Goldbach et al., 2019) was
127 used as control (C2). For lipase, binding site with a radius of 15 Å and coordinates x: 8.02469, y:
128 23.5388, z: 55.7064 was created. A known lipase inhibitory peptide, YFS (Stefanucci et al., 2019)
129 was used as control (C3).

130 **2.5. Statistical analyses**

131 Triplicate measurements were performed for enzyme inhibition determinations. Statistical
132 significance was analyzed using SPSS 22.0 (IL, USA).

133

3. Results and discussion

3.1. *In vitro* multi-enzyme inhibitory activities of peptides

As shown in **Fig. 1**, the peptides strongly inhibited ACE (52.2−78.8%) followed by α-amylase (16.3−27.2%), and least for pancreatic lipase (5.3−17.0%). It suggests that *C. frondosa* could be source material to produce enzyme-inhibitory peptides. Other closely related species recently reported with ACE inhibitory peptide activities include *Stichopus japonicus* and *Holothuria atra* (Dewi, Patantis, Fawzya, Irianto, & Sa'diah, 2020; Zhong, Sun, Yan, Lin, Liu, & Cao, 2018). However, peptides derived from sea cucumber with α-amylase and lipase inhibitory activities have not been reported.

ACE inhibitory activity (**Fig. 1a**) showed that the peptides with relatively low MW, i.e., <2 kDa and 2-3 kDa, had significantly high ACE inhibitory activity ($p < 0.05$) which agreed with previous findings on *Acaudina molpadioidea* peptides (Zhao, Li, Liu, Dong, Zhao, & Zeng, 2007). Peptide fractions $A_{<2}$ and $T_{<2}$ (MW <2 kDa, 2 mg/mL) from *C. frondosa* inhibited ACE activity by 78.8% and 65.4%, respectively, which were higher than their counterparts generated from *H. atra* (57.4%, MW <3 kDa, 1 mg/mL) (Dewi et al., 2020) and *S. japonicus* gonads (50%, MW <3 kDa, 1.32 mg/mL) (Zhong et al., 2018). Previously found peptides exhibiting high α-amylase inhibitory activity were mainly from plant sources (Awosika & Aluko, 2019), and only a few from aquatic sources, e.g., shrimp and red seaweed (Admassu et al., 2018; Yuan, Li, Pan, Wang, & Chen, 2018). This study indicated that sea cucumber is a potential marine source of α-amylase inhibitory peptides. Peptide fractions $A_{<2}$ and $T_{<2}$ had 27.2% and 24.1% α-amylase inhibitory activities, respectively (**Fig. 1b**). Collagen is the main protein component in sea cucumber, and a study on camel skin collagen hydrolysates also found peptides with potent ACE and pancreatic α-amylase inhibitory activities (Mudgil, Jobe, Kamal, Alameri, Al Ahbabi, &

Maqsood, 2019). Inhibition effect of the peptides on pancreatic lipase was low (**Fig. 1c**) with $A_{<2}$ and $T_{<2}$ showing 18.3% and 15.3% inhibitory activities against lipase, respectively. Similarly, peptides produced from yellow field pea showed both α-amylase and lipase inhibitory activities, and 50% reduction in lipase activity was achieved by a high concentration (4–12 mg/mL) of peptides (Awosika et al., 2019).

3.2. *In silico* analyses of peptide properties

Peptide sequences obtained from *de novo* sequencing with both average local confident (ALC) values ≥90% and local confidence (LC) values ≥70% were selected (**Table 1**). There were 11 sequences in $A_{<2}$, and 32 sequences in $T_{<2}$. All peptides consisted of 5–9 amino acids. Peptides in $A_{<2}$ had pI values from 5.10 to 11.29, and 46% were water soluble, while peptides in $T_{<2}$ had broader pI values from 3.85 to 11.39, and 72% showed high water solubility. Potential anti-health properties were predicted that no peptide was toxic and allergenic, suggesting the peptides had low possibility to pose a food safety issue.

The potential bioactivity of each peptide was assessed (**Table 1**). Peptide YDWRF (No. 1 in $A_{<2}$) had the highest possibility to be the most bioactive, and peptide WDLFR (No. 4 in $A_{<2}$, No. 30 in $T_{<2}$) had the 2nd highest score. In total, 55% peptides in $A_{<2}$ had bioactive potential ≥0.8, but only 9% peptides in $T_{<2}$ fraction had bioactivity ≥0.8, suggesting that alcalase produced more bioactive peptides than trypsin. Specifically, 100% of peptides in $A_{<2}$ fraction and 87.5% of peptides in $T_{<2}$ fraction were found with ACE inhibitory fragments. The composition of certain amino acids, including aromatic, hydrophobic, basic, and positively-charged amino acids contribute to ACE inhibitory activity (Lee & Hur, 2017). In the study, peptide EVPLFR with parameter A value of 1.0 was found with ACE inhibitory fragments EV, VP, PL, LF, LFR and FR that comprised of aliphatic amino acids (V, L), aromatic amino acids (F, R, P), and they

provided high affinity towards the active site of ACE due to hydrophobicity (Lee et al., 2017; Li, Le, Shi, & Shrestha, 2004). No α-amylase and lipase inhibitory fragments were found in peptides, which was due to the lack of relevant dataset in BIOPEP-UWM. Admassu et al. (2018) reported 2 α-amylase inhibitory peptides, GGSK and ELS, produced from red seaweed. Ngoh et al. (2016) reported 7 α-amylase inhibitory peptides from Pinto beans that possessed amino acids such as L, P, G and F, similar to the data from this work. Findings on lipase inhibitory peptides are still insufficient. ε-Polylysine (25–30 K residues) is commercially used as food additives in Japan because of its inhibition against human and porcine pancreatic lipase. Tripeptides containing high content of R residues were synthesized and exhibited strong inhibition against lipase (Stefanucci et al., 2019). Peptides NPVWKRK and CANPHELPNK derived from *Spirulina platensis* decreased the accumulation of triglyceride by binding pancreatic lipase (Fan, Cui, Zhang, & Zhang, 2018). In this study, several peptides containing these characteristic amino acids that were responsible for the inhibition of α-amylase and lipase were observed (**Fig. 1**).

3.3 Inhibition mechanisms of peptides inhibiting multi-enzymes

According to the (−)CDOCKER energy data (**Table 1)** that present the overall energy consumed by peptide as inhibitor when bound with enzyme active site, all the produced peptides possessed inhibitory activities against ACE and pancreatic α-amylase. Six peptides were able to inhibit ACE, pancreatic α-amylase and lipase. Peptides generated by trypsin generally exhibited higher inhibitory activities than alcalase produced peptides, which differed with the results obtained using peptide database in subsection 3.2. For each peptide, the data from molecular docking only matched those returned from online tools to a small extent. It suggested that the structure of the peptides played a key role in inhibiting enzymes. The control peptide C1, PRY, is a strong competitive inhibitor of ACE by forming H-bond (Fu et al., 2017) and it showed a

docking energy of −57.7345. All peptides produced from *C. frondosa* had lower docking energy values, indicating they were stronger ACE inhibitors than PRY. The control peptide C2, YPYSCWVRH, is a selective and competitive inhibitor against α-amylase (Goldbach et al., 2019), and its binding to pancreatic α-amylase consumed energy of −134.391. Peptides FENLLEELK, FNTDSALER, SYNELLTK in this study appeared to be stronger α-amylase inhibitors than C2 as they consumed much lower energies. The control tripeptide C3, YFS, showed a CDOCKER energy of −61.3976 against pancreatic lipase. Among the 6 peptides successfully docked onto lipase, peptide APFPLR had a similar docking energy value to C3, and the other 5 peptides appeared to be stronger inhibitors than C3. The peptides that failed in docking with lipase were too large to fit in lipase active site. The structure–function relationship of multi-enzyme inhibitory peptide was illustrated by peptide FENLLEELK (**Fig. S1**a), which had robust inhibitory activities against ACE and pancreatic α-amylase, as well as peptide APFPLR (**Fig. S1**b) which showed moderate inhibitory activities against ACE, pancreatic α-amylase and lipase.

3.3.1. Inhibition mechanisms of peptide FENLLEELK

The overall structure of human ACE is in an ellipsoid shape with a central groove that extends to the internal enzyme molecule, and peptide FENLLEELK buried in the groove (**Fig. 2a**). It had an extended conformation that enabled its access to ACE active site crevice (**Fig. 2b**); thus, was able to prevent zinc, the essential cofactor of ACE, from binding with the conserved HEXXH zinc binding motif in ACE (His_{383}, His_{387}, Glu_{411}) (Natesh, Schwager, Sturrock, & Acharya, 2003) located at the bottom of peptide–ACE interaction surface. Each residue in the peptide participated in the interaction with atoms in ACE active site (**Fig. 2c**). The F residue on the N-terminal of the peptide formed desirable carbon hydrogen bonds with Asn_{66} (2.45 Å),

226 Try_{62} (2.45 Å) but the interaction was slightly weakened by unfavorable positive-positive
227 interaction with Arg_{124} (4.67 Å) (Zhao, Zhang, Yu, Ding, & Liu, 2020). The K residue on the
228 peptide C-terminal formed attractive charge interaction with Asp_{121} (4.35 Å) and a salt bridge
229 with Glu_{123} (1.9 Å) via lysyl side chain, apart from attractive charge interaction with Arg_{124} (5.38
230 Å) and a conventional H-bond with Trp_{220} (2.87 Å) from the $-COO^-$ group. FENLLEELK had 3
231 E residues and 3 L residues. The carboxyl side chain from E residues formed strong electrostatic
232 interactions with Arg_{124}, His_{410}, Arg_{522}, Lys_{118}, as well as a conventional H-bond with Arg_{522}
233 which was reported as the chloride ion ligand for ACE activation for substrate hydrolysis
234 (Natesh et al., 2003). The isobutyl group of L residues formed hydrophobic interactions with
235 Trp_{59}, Phe_{391} and Val_{518}. The interactions between peptide and ACE active site including H-bond,
236 electrostatic and hydrophobic effects were intense.

237 Peptide FENLLEELK was also buried in the active site cleft of human pancreatic α-
238 amylase as seen from the top view of the surface (**Fig. 3a**). Compared to the pose when docking
239 with ACE (**Fig. 2b**), the same peptide formed a more compact pose in a unique lariat fold when
240 interacting with lipase (**Fig. 3b**). Previous research found that lariat-type peptides were potent
241 and highly selective to α-amylase over other glycosidases (Jongkees, Caner, Tysoe, Brayer,
242 Withers, & Suga, 2017). The six residues on peptide N-terminal, i.e., FENLLE formed a head-to-
243 side chain macrocycle, while the C-terminal residue K stretched to the base of the active site
244 cleft to form interactions with atoms in α-amylase active pocket. The macrocycle composed of
245 six amino acids was stabilized by various intermolecular H-bond and charge interactions (**Fig. 3c**)
246 and was responsible for a few interactions with the α-amylase active site. The F residue formed
247 pi-charge electrostatic bond with Trp_{59}; the N residue formed conventional H-bond with Val_{354}
248 (2.61 Å); the L residue formed electrostatic interactions with Val_{354} (4.34 Å) and His_{305} (4.88 Å);

249 however, the E residue formed an undesirable charge repulsion with negatively charged Asp_{356}
250 (5.3 Å) (**Fig. 3d**). The "tail" of the lariat peptide residue K towards the end of active site pocket,
251 was the one contributing the most to the inhibition, due to the large number of interactions to the
252 active atoms especially the catalytic triad in α-amylase (Asp_{197}–Asp_{300}–Glu_{233}). Although it
253 formed an unfavorable donor-donor clash with Ala_{198}, the $-NH_3$ group on the side chain made
254 two conventional H-bonds (2.38 Å, 2.7 Å) and one attractive charge interaction (4.33 Å) with
255 Asp_{197}, the catalytic nucleophile of α-amylase, and one electrostatic interaction (4.75 Å) with
256 Asp_{300}, as well as one conventional H-bond (1.96 Å) and one salt bridge (2.07 Å) with Glu_{233}
257 which is the catalytic acid-base of α-amylase (Goldbach et al., 2019).
258 3.3.2. Inhibition mechanisms of peptide APFPLR
259 The pose of APFPLR in ACE active site was extended to block the entrance for substrate
260 binding. The binding between peptide and non-catalytic residues in ACE active site was
261 facilitated by electrostatic interactions, hydrophobic interactions and H-bonds (**Fig. S2a**).
262 Conversely, peptide APFPLR engaged intensively with pancreatic α-amylase. It formed a curled
263 structure among the A, P, F, P residues and stretched its R residue to the bottom of the α-amylase
264 active site with its guanidino group in the side chain interacting with the α-amylase catalytic triad
265 with both H-bonds and attractive charge interactions (**Fig. S2b**).
266 Peptide APFPLR was one of the several peptides that docked on human pancreatic lipase, a
267 receptor used in this study in an activated form and in complex with co-lipase, an amphiphilic
268 protein facilitating the opening of the lid domain (**Fig. 4a**) to allow efficient lipolysis at a hostile
269 lipid-water interface (Stefanucci et al., 2019). APFPLR formed a stretched pose with its C-
270 terminal towards the end of the interaction surface to occupy the narrow and shallow active site
271 groove of lipase (**Fig. 4b**), and its catalytic triad Ser_{152}–Asp_{176}–His_{263} was blocked at the bottom

of the interaction surface of lipase–peptide complex (**Fig. 4c**). A strong interaction network was formed between the peptide and the residues in lipase active pocket (**Fig. 4d**), and the comprised residues A, P and L are aliphatic that favored the binding with lipase active site. The A residue on peptide N-terminal formed H-bonds with Thr_{21} and Glu_{22}. Other residues in the peptide mainly made hydrophobic interactions with lipase active site atoms. For example, the pyrrolidine side chain of P residue made a hydrophobic interaction towards Cys_{181}; the benzyl side chain of F residue made hydrophobic interactions with Ile_{209} and Val_{210}; and the L residue formed hydrophobic interactions with Phe_{77}, Pro_{180}, Tyr_{114}, Ala_{178}, among which the Phe_{77} is the H-bond donor and electrostatic stabilizer to form oxyanion hole for substrate hydrolysis (Eydoux et al., 2008). The R residue on C-terminal interacted with Asp_{79} and Phe_{77} with conventional H-bond and/or charge-charge interaction via its $-NH_3$ group. Moreover, the C-terminal ($-COO^-$) made a carbon H-bond (2.4 Å) and a charge-charge interaction (4.82 Å) with His_{263}, which is in the catalytic triad to be attacked by Asp_{176} and acts as a general base in lipase catalysis (Eydoux et al., 2008).

4. Conclusions

Peptides derived from *C. frondosa* inhibited ACE, α-amylase and lipase based on *in vitro* and *in silico* data. Peptide with the same sequence adjusted its conformational structure to bind towards the active sites of multi-enzymes. FENLLEELK exhibited potent inhibitory activities against ACE and α-amylase by forming different poses and weak interactions. APFPLR inhibited pancreatic lipase due to the amphipathicity of the constituent amino acids, structural features and intense interactions with catalytic residues. This research illustrated the molecular mechanisms and structure–function relationship of multi-enzyme inhibitory peptides against different

295 enzymes.

296

297 **Declaration of Competing Interest**

298 The authors declare no conflict of interest.

299

300 **Acknowledgements**

301 This work was funded by Natural Sciences and Engineering Research Council of Canada
302 (NSERC) Discovery Grants.

303

304 **References**

305 Admassu, H., Gasmalla, M. A., Yang, R., & Zhao, W. (2018). Identification of bioactive
306 peptides with α-amylase inhibitory potential from enzymatic protein hydrolysates of red
307 seaweed (*Porphyra* spp). *Journal of Agricultural and Food Chemistry, 66*(19), 4872-
308 4882.

309 Awosika, T. O., & Aluko, R. E. (2019). Inhibition of the *in vitro* activities of α-amylase, α-
310 glucosidase and pancreatic lipase by yellow field pea (*Pisum sativum* L.) protein
311 hydrolysates. *International Journal of Food Science & Technology, 54*(6), 2021-2034.

312 Cardullo, N., Muccilli, V., Pulvirenti, L., Cornu, A., Pouységu, L., Deffieux, D., Quideau, S., &
313 Tringali, C. (2020). C-glucosidic ellagitannins and galloylated glucoses as potential
314 functional food ingredients with anti-diabetic properties: A study of α-glucosidase and α-
315 amylase inhibition. *Food Chemistry, 313*, 126099.

316 Daliri, E. B.-M., Lee, B. H., & Oh, D. H. (2018). Current trends and perspectives of bioactive
317 peptides. *Critical Reviews in Food Science and Nutrition, 58*(13), 2273-2284.

Dewi, A. S., Patantis, G., Fawzya, Y. N., Irianto, H. E., & Sa'diah, S. (2020). Angiotensin-converting enzyme (ACE) inhibitory activities of protein hydrolysates from Indonesian sea cucumbers. *International Journal of Peptide Research and Therapeutics, 26*, 2485–2493.

Eydoux, C., Spinelli, S., Davis, T. L., Walker, J. R., Seitova, A., Dhe-Paganon, S., De Caro, A., Cambillau, C., & Carrière, F. d. r. (2008). Structure of human pancreatic lipase-related protein 2 with the lid in an open conformation. *Biochemistry, 47*(36), 9553-9564.

Fan, X., Cui, Y., Zhang, R., & Zhang, X. (2018). Purification and identification of anti-obesity peptides derived from *Spirulina platensis*. *Journal of Functional Foods, 47*, 350-360.

Fu, Y., Alashi, A. M., Young, J. F., Therkildsen, M., & Aluko, R. E. (2017). Enzyme inhibition kinetics and molecular interactions of patatin peptides with angiotensin I-converting enzyme and renin. *International Journal of Biological Macromolecules, 101*, 207-213.

Goldbach, L., Vermeulen, B. J., Caner, S., Liu, M., Tysoe, C., van Gijzel, L., Yoshisada, R., Trellet, M., van Ingen, H., & Brayer, G. D. (2019). Folding then binding vs folding through binding in macrocyclic peptide inhibitors of human pancreatic α-amylase. *ACS Chemical Biology, 14*(8), 1751-1759.

Gupta, S., Kapoor, P., Chaudhary, K., Gautam, A., Kumar, R., Raghava, G. P., & Consortium, O. S. D. D. (2013). *In silico* approach for predicting toxicity of peptides and proteins. *PloS One, 8*(9), e73957.

Han, R., Maycock, J., Murray, B. S., & Boesch, C. (2019). Identification of angiotensin converting enzyme and dipeptidyl peptidase-IV inhibitory peptides derived from oilseed proteins using two integrated bioinformatic approaches. *Food Research International, 115*, 283-291.

341 Huang, Y.-L., Chow, C.-J., & Tsai, Y.-H. (2012). Composition, characteristics, and *in-vitro*
342 physiological effects of the water-soluble polysaccharides from Cassia seed. *Food*
343 *Chemistry, 134*(4), 1967-1972.
344 Jongkees, S. A., Caner, S., Tysoe, C., Brayer, G. D., Withers, S. G., & Suga, H. (2017). Rapid
345 discovery of potent and selective glycosidase-inhibiting *de novo* peptides. *Cell Chemical*
346 *Biology, 24*(3), 381-390.
347 Kang, N. J., Jin, H.-S., Lee, S.-E., Kim, H. J., Koh, H., & Lee, D.-W. (2020). New approaches
348 towards the discovery and evaluation of bioactive peptides from natural resources.
349 *Critical Reviews in Environmental Science and Technology, 50*(1), 72-103.
350 Lee, S. Y., & Hur, S. J. (2017). Antihypertensive peptides from animal products, marine
351 organisms, and plants. *Food Chemistry, 228*, 506-517.
352 Li, G.-H., Le, G.-W., Shi, Y.-H., & Shrestha, S. (2004). Angiotensin I–converting enzyme
353 inhibitory peptides derived from food proteins and their physiological and
354 pharmacological effects. *Nutrition Research, 24*(7), 469-486.
355 Minkiewicz, P., Iwaniak, A., & Darewicz, M. (2019). BIOPEP-UWM database of bioactive
356 peptides: Current opportunities. *International Journal of Molecular Sciences, 20*(23),
357 5978.
358 Mudgil, P., Jobe, B., Kamal, H., Alameri, M., Al Ahbabi, N., & Maqsood, S. (2019). Dipeptidyl
359 peptidase-IV, α-amylase, and angiotensin I converting enzyme inhibitory properties of
360 novel camel skin gelatin hydrolysates. *LWT, 101*, 251-258.
361 Natesh, R., Schwager, S. L., Sturrock, E. D., & Acharya, K. R. (2003). Crystal structure of the
362 human angiotensin-converting enzyme–lisinopril complex. *Nature, 421*(6922), 551-554.

Ngoh, Y.-Y., & Gan, C.-Y. (2016). Enzyme-assisted extraction and identification of antioxidative and α-amylase inhibitory peptides from Pinto beans (*Phaseolus vulgaris* cv. Pinto). *Food Chemistry, 190*, 331-337.

Rajan, L., Palaniswamy, D., & Mohankumar, S. K. (2020). Targeting Obesity with plant-derived pancreatic lipase inhibitors: A comprehensive review. *Pharmacological Research, 155*, 104681.

Stefanucci, A., Luisi, G., Zengin, G., Macedonio, G., Dimmito, M. P., Novellino, E., & Mollica, A. (2019). Discovery of arginine-containing tripeptides as a new class of pancreatic lipase inhibitors. *Future Medicinal Chemistry, 11*(1), 5-19.

Toopcham, T., Mes, J. J., Wichers, H. J., Roytrakul, S., & Yongsawatdigul, J. (2017). Bioavailability of angiotensin I-converting enzyme (ACE) inhibitory peptides derived from *Virgibacillus halodenitrificans* SK1-3-7 proteinases hydrolyzed tilapia muscle proteins. *Food Chemistry, 220*, 190-197.

Wang, X., Chen, H., Fu, X., Li, S., & Wei, J. (2017). A novel antioxidant and ACE inhibitory peptide from rice bran protein: Biochemical characterization and molecular docking study. *LWT, 75*, 93-99.

Yuan, G., Li, W., Pan, Y., Wang, C., & Chen, H. (2018). Shrimp shell wastes: Optimization of peptide hydrolysis and peptide inhibition of α-amylase. *Food Bioscience, 25*, 52-60.

Zhang, T., Li, M., Fu, X., & Mou, H. (2019). Purification and charicterization of angiotensin I-converting enzyme (ACE) inhibitory peptides with specific structure X-Pro. *European Food Research and Technology, 245*(8), 1743-1753.

Zhang, Y., Aryee, A. N., & Simpson, B. K. (2020a). Current role of *in silico* approaches for food enzymes. *Current Opinion in Food Science, 31*, 63-70.

386 Zhang, Y., He, S., Bonneil, É., & Simpson, B. K. (2020b). Generation of antioxidative peptides
387 from Atlantic sea cucumber using alcalase versus trypsin: *In vitro* activity, *de novo*
388 sequencing, and *in silico* docking for *in vivo* function prediction. *Food Chemistry, 306*,
389 125581.
390 Zhao, W., Zhang, D., Yu, Z., Ding, L., & Liu, J. (2020). Novel membrane peptidase inhibitory
391 peptides with activity against angiotensin converting enzyme and dipeptidyl peptidase IV
392 identified from hen eggs. *Journal of Functional Foods, 64*, 103649.
393 Zhao, Y., Li, B., Liu, Z., Dong, S., Zhao, X., & Zeng, M. (2007). Antihypertensive effect and
394 purification of an ACE inhibitory peptide from sea cucumber gelatin hydrolysate.
395 *Process Biochemistry, 42*(12), 1586-1591.
396 Zhong, C., Sun, L.-C., Yan, L.-J., Lin, Y.-C., Liu, G.-M., & Cao, M.-J. (2018). Production,
397 optimisation and characterisation of angiotensin converting enzyme inhibitory peptides
398 from sea cucumber (*Stichopus japonicus*) gonad. *Food & Function, 9*(1), 594-603.

Table 1

The sequences, physiochemical properties, bioactivities, safety and docking energies of inhibitory peptides.

No.	Peptide sequence	*De novo* sequencing		Physicochemical property		Bioactivity (Peptide Ranker)	Enzyme inhibitory activity			Safety		(–)CDOCKER Energy		
							ACE		α-amylase	Toxicity	Allergenicity			
		ALC (%)	LC (%)	pI	H_2O solubility		Location of fragments	Parameter A				ACE	α-amylase	lipase
Alcalase-produced peptides														
1	YDWRF	97	96 97 98 98 97	6.36	Good	0.965565	YDWRF	0.2000	---	No	---	112.639	101.845	F
2	VVLLPLR	95	95 96 100 100 88 94 93	10.8	Poor	0.375063	VVLLPLR	0.4286	---	No	---	112.618	100.133	F
3	LDLPLR	95	92 90 97 97 98 95	6.64	Good	0.601238	LDLPLR	0.5000	---	No	---	107.664	117.235	F
4	WDLFR	94	94 86 98 97 94	6.52	Good	0.956441	WDLFR	0.6000	---	No	---	88.8559	81.5657	F
5	ELPPHFL	93	90 88 96 97 95 93 96	5.10	Poor	0.821660	ELPPHFL	0.4286	---	No	---	108.682	84.4674	74.5224
6	APFPLR	92	84 88 93 93 98 95	10.9	Poor	0.947738	APFPLR	0.8333	---	No	---	81.5545	70.4191	60.7478
7	VPFLPR	92	90 87 96 97 92 90	10.8	Poor	0.797496	VPFLPR	0.3333	---	No	---	80.8358	75.3007	F
8	PLQLRP	91	96 99 96 94 81 82	11.3	Good	0.599230	PLQLRP	0.8333	---	No	---	85.5900	76.1232	F
9	TEFHLL	91	90 96 73 91 97 97	5.10	Poor	0.395475	TEFHLL	0.5000	---	No	---	129.975	104.348	F
10	PVFPLR	90	96 97 97 74 86 92	11.3	Poor	0.864694	PVFPLR	0.6667	---	No	---	86.2038	68.7906	F
11	EVPLRFW	90	88 79 94 98 88 90 93	6.86	Good	0.830047	EVPLRFW	0.7143	---	No	---	112.161	95.4367	F
Trypsin-produced peptides														
1	VELWR	97	93 100 98 98 97	6.84	Good	0.298764	VELWR	0.4000	---	No	---	107.935	105.588	F
2	WALLVDAPR	96	90 99 100 99 96 96 97 98 97	6.52	Poor	0.419358	WALLVDAPR	0.4444	---	No	---	141.922	126.433	F
3	LLVNFR	96	98 99 96 92 96 97	10.8	Poor	0.429748	LLVNFR	0.3333	---	No	---	121.291	116.337	F
4	VVNLWR	96	98 97 94 94 96 97	10.8	Poor	0.378438	VVNLWR	0.1667	---	No	---	114.319	110.854	F
5	QAPVKPR	96	95 98 98 95 96 96 95	11.4	Good	0.422813	QAPVKPR	0.7143	---	No	---	104.272	97.6040	F
6	LQLWR	96	94 94 97 96 99	10.8	Good	0.704684	LQLWR	0.4000	---	No	---	103.409	108.075	F
7	FPSLVGR	95	96 97 99 100 98 95 82	10.6	Poor	0.643490	FPSLVGR	0.4286	---	No	---	105.061	99.8073	F
8	LEEQSR	95	94 98 98 88 95 98	4.15	Good	0.0511313	LEEQSR	0.1667	---	No	---	148.099	120.492	F

9	WLDVLR	95	96 95 93 93 97 96	6.52	Good	0.631447	WLDVLR	0.3333	---	No	---	123.579	121.832	F
10	LLMELR	95	97 96 88 96 97 97	6.86	Good	0.345431	LLMELR	0.3333	---	No	---	131.147	121.354	F
11	LLLEMEK	94	79 97 97 98 95 99 98	4.15	Good	0.0988306	LLLEMEK	0.2857	---	No	---	159.526	131.090	F
12	LLELLK	94	89 89 98 96 99 97	6.85	Good	0.157782	LLELLK	---	---	No	---	135.126	117.700	F
13	FENLLEELK	93	79 93 95 91 96 98 98 98 98	3.85	Good	0.163453	FENLLEELK	0.1111	---	No	---	205.065	167.002	F
14	MNLPFR	93	86 93 96 93 96 97	10.6	Poor	0.902172	MNLPFR	0.3333	---	No	---	110.060	105.355	F
15	FVLELR	93	82 92 96 98 98 96	6.62	Good	0.319959	FVLELR	0.1667	---	No	---	135.643	120.277	F
16	EYVFR	93	92 90 93 96 97	6.81	Good	0.351391	EYVFR	0.8000	---	No	---	113.542	119.242	F
17	LNLDLLR	93	92 91 94 90 92 96 96	6.64	Good	0.457278	LNLDLLR	0.2857	---	No	---	144.478	131.423	93.0810
18	SNNVLFR	93	85 85 97 94 98 98 96	10.6	Poor	0.673915	SNNVLFR	0.4286	---	No	---	136.041	118.587	F
19	LENVLR	93	91 96 86 90 97 98	6.86	Good	0.126053	LENVLR	0.1667	---	No	---	137.731	124.212	F
20	VMQDQVLR	93	90 95 91 91 89 93 99 97	6.61	Good	0.222451	VMQDQVLR	0.1250	---	No	---	159.909	137.249	F
21	KVSWR	92	84 95 92 93 97	11.4	Good	0.330550	KVSWR	---	---	No	---	107.854	112.654	F
22	SYNELLTK	92	84 86 93 95 86 97 99 97	6.58	Good	0.213744	SYNELLTK	0.2500	---	No	---	169.344	148.307	F
23	LLQLAR	92	95 97 86 91 90 92	10.8	Poor	0.252639	LLQLAR	0.5000	---	No	---	108.805	109.644	F
24	FNTDSALER	92	82 82 97 96 88 89 98 100 96	3.93	Good	0.191898	FNTDSALER	---	---	No	---	174.249	159.707	F
25	LNFEPR	91	91 87 92 97 89 95	6.86	Good	0.470901	LNFEPR	0.8333	---	No	---	129.363	101.454	72.3177
26	TTDVLR	91	85 82 93 94 98 96	6.33	Good	0.0895658	TTDVLR	0.1667	---	No	---	124.179	119.971	94.1367
27	FEQFFK	91	87 96 97 98 95 72	6.61	Good	0.833484	FEQFFK	---	---	No	---	148.119	122.455	F
28	FVTVLR	90	89 89 86 88 96 96	10.6	Poor	0.259446	FVTVLR	0.1667	---	No	---	116.674	113.835	F
29	MANLQR	90	88 92 90 92 88 95	10.6	Poor	0.257394	MANLQR	0.1667	---	No	---	128.732	114.027	82.5811
30	WDLFR	90	82 85 96 94 95	6.52	Good	0.956441	WDLFR	0.6000	---	No	---	112.303	115.031	F
31	ELFDPR	90	92 86 89 91 89 93	3.93	Good	0.561531	ELFDPR	0.3333	---	No	---	127.572	98.7788	F
32	EVPLFR	90	92 85 92 88 87 96	6.86	Good	0.535712	EVPLFR	1.0000	---	No	---	113.853	98.6151	F

Notes: In the “Enzyme inhibitory activity” category, the location of fragments with ACE inhibitory bioactivity were presented with blue underlines for each peptide. The “---” means no data returned from the online tools. The “F” in the “(−)CDOCKER Energy” category means the failure of molecular docking of the peptide with human pancreatic lipase.

Figure Captions

Fig. 1. ACE inhibitory activity **(a)**, pancreatic α-amylase inhibitory activity **(b)**, and pancreatic lipase inhibitory activity **(c),** of peptides produced via alcalase (A) or trypsin (T) hydrolysis (MW ranges of <10 kDa, 10–5 kDa, <5 kDa, 5–3 kDa, <3 kDa, 3–2 kDa and <2 kDa). Different letters in alcalase (A)-produced peptides (a, b, c, d, e) or trypsin (T)-produced peptides (a', b', c') means significant difference ($p < 0.05$). Significance levels of $*p < 0.05$, $**p < 0.01$ and $***p < 0.001$ were for A- versus T-produced peptides.

Fig. 2. Molecular interaction between inhibitory peptide FENLLEELK and human ACE. Top view of FENLLEELK binding with ACE **(a)**. Molecular surface (H-bond donor and H-bond acceptor in pink and green, respectively) between peptide and ACE active site (peptide molecule in stick and colored by element; key residues of ACE zinc-binding motif in yellow stick) **(b)**. Interactions of ACE–peptide complex (interacting residues of ACE shown in different color based on different interactions) **(c)**.

Fig. 3. Molecular interaction between inhibitory peptide FENLLEELK and human pancreatic α-amylase. Top view of FENLLEELK binding with α-amylase **(a)**. Molecular surface (H-bond donor and H-bond acceptor in pink and green, respectively) between peptide and α-amylase active site (peptide molecule in stick and colored by element; key residues of α-amylase in yellow stick) **(b)**. FENLLEELK in lariat shape **(c)**. Interactions of α-amylase–peptide complex (interacting residues of α-amylase shown in different color based on different interactions) **(d)**.

Fig. 4. Molecular interaction between inhibitory peptide APFPLR and human pancreatic lipase. Pancreatic lipase–co-lipase–peptide complex **(a)**. Top view of APFPLR binding with lipase **(b)**. Molecular surface (H-bond donor and H-bond acceptor in pink and green, respectively) between peptide and lipase active site (peptide molecule in stick and colored by element; key residues of lipase in yellow stick **(c)**. Interactions of lipase–peptide complex (interacting residues of lipase shown in different color based on different interactions) **(d)**.

Fig. 1

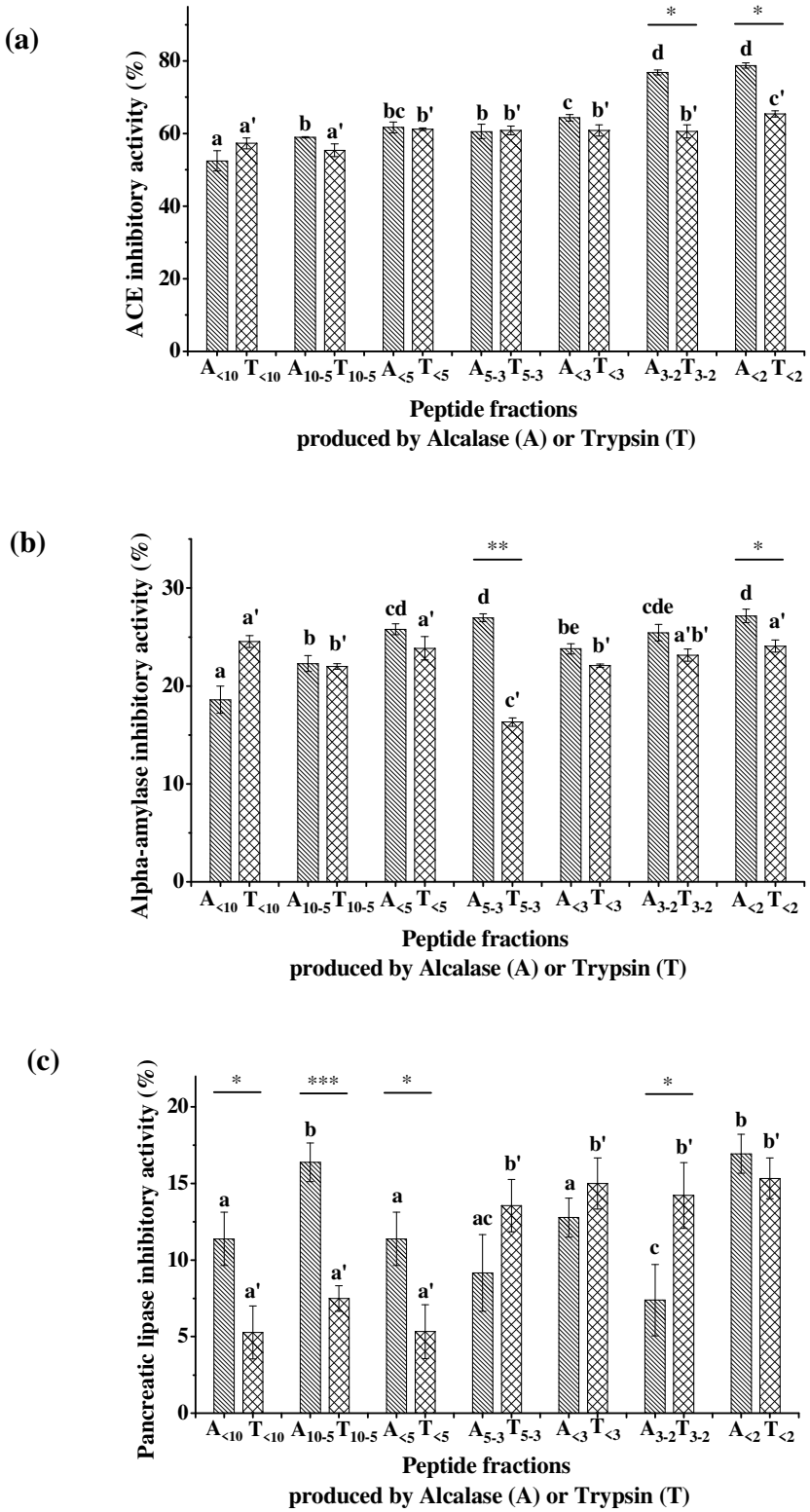
(a)
ACE inhibitory activity (%)
0
20
40
60
80
*
*
a
a'
b
a'
bc
b'
b
b'
c
b'
d
b'
d
c'
A<10 T<10 A10-5 T10-5 A<5 T<5 A5-3 T5-3 A<3 T<3 A3-2 T3-2 A<2 T<2
Peptide fractions
produced by Alcalase (A) or Trypsin (T)
(b)
Alpha-amylase inhibitory activity (%)
0
10
20
30
**
*
a
a'
b
b'
cd
a'
d
c'
be
b'
cde
a'b'
d
a'
A<10 T<10 A10-5 T10-5 A<5 T<5 A5-3 T5-3 A<3 T<3 A3-2 T3-2 A<2 T<2
Peptide fractions
produced by Alcalase (A) or Trypsin (T)
(c)
Pancreatic lipase inhibitory activity (%)
0
5
10
15
20
*
***
*
*
a
a'
b
a'
a
a'
ac
b'
a
b'
c
b'
b
b'
A<10 T<10 A10-5 T10-5 A<5 T<5 A5-3 T5-3 A<3 T<3 A3-2 T3-2 A<2 T<2
Peptide fractions
produced by Alcalase (A) or Trypsin (T)

Fig. 2

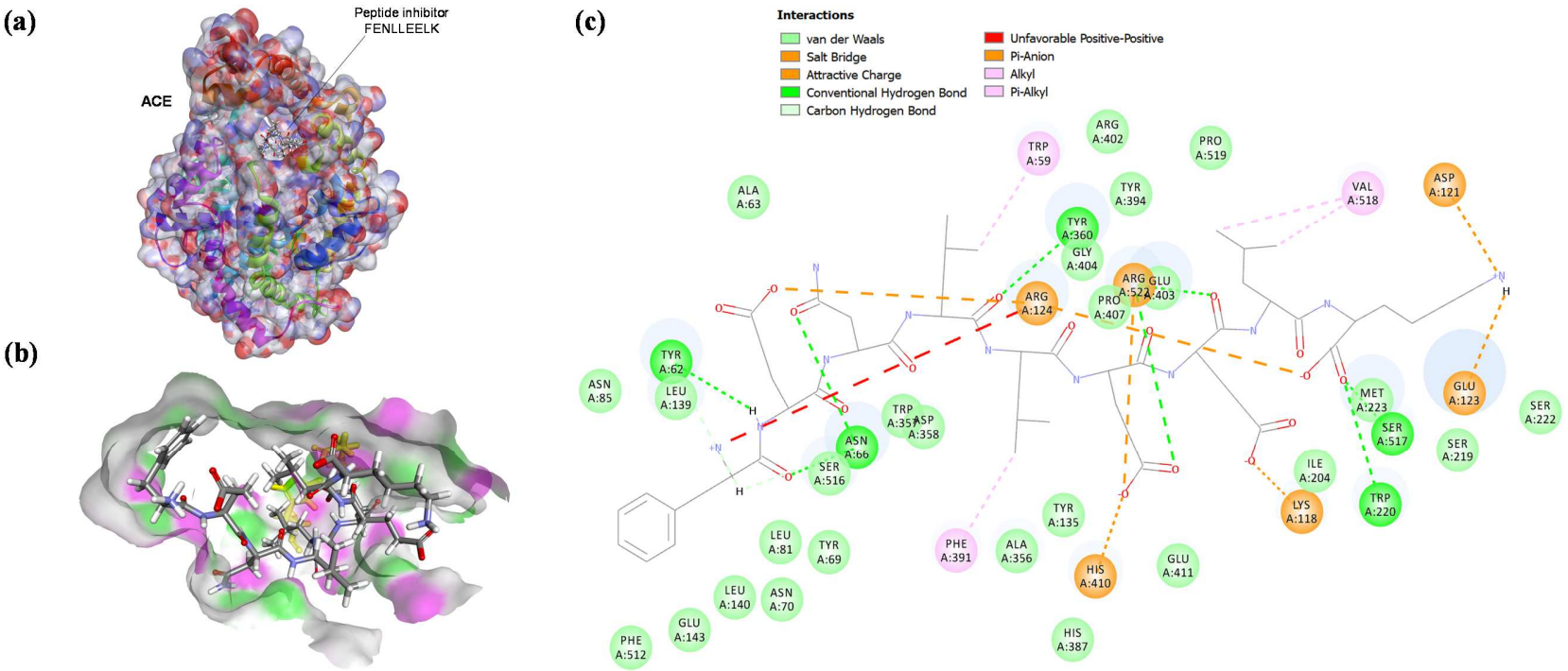
(a)
Peptide inhibitor
FENLLEELK
ACE
(b)
(c)
Interactions
van der Waals
Salt Bridge
Attractive Charge
Conventional Hydrogen Bond
Carbon Hydrogen Bond
Unfavorable Positive-Positive
Pi-Anion
Alkyl
Pi-Alkyl
ARG A:402
TRP A:59
PRO A:519
ALA A:63
TYR A:394
VAL A:518
ASP A:121
TYR A:360
GLY A:404
ARG A:522
GLU A:403
ARG A:124
PRO A:407
TYR A:62
LEU A:139
ASN A:85
TRP A:357
ASP A:358
ASN A:66
SER A:516
MET A:223
SER A:517
GLU A:123
SER A:222
SER A:219
ILE A:204
LYS A:118
TRP A:220
TYR A:135
LEU A:81
TYR A:69
PHE A:391
ALA A:356
HIS A:410
GLU A:411
LEU A:140
ASN A:70
GLU A:143
PHE A:512
HIS A:387

Fig. 3

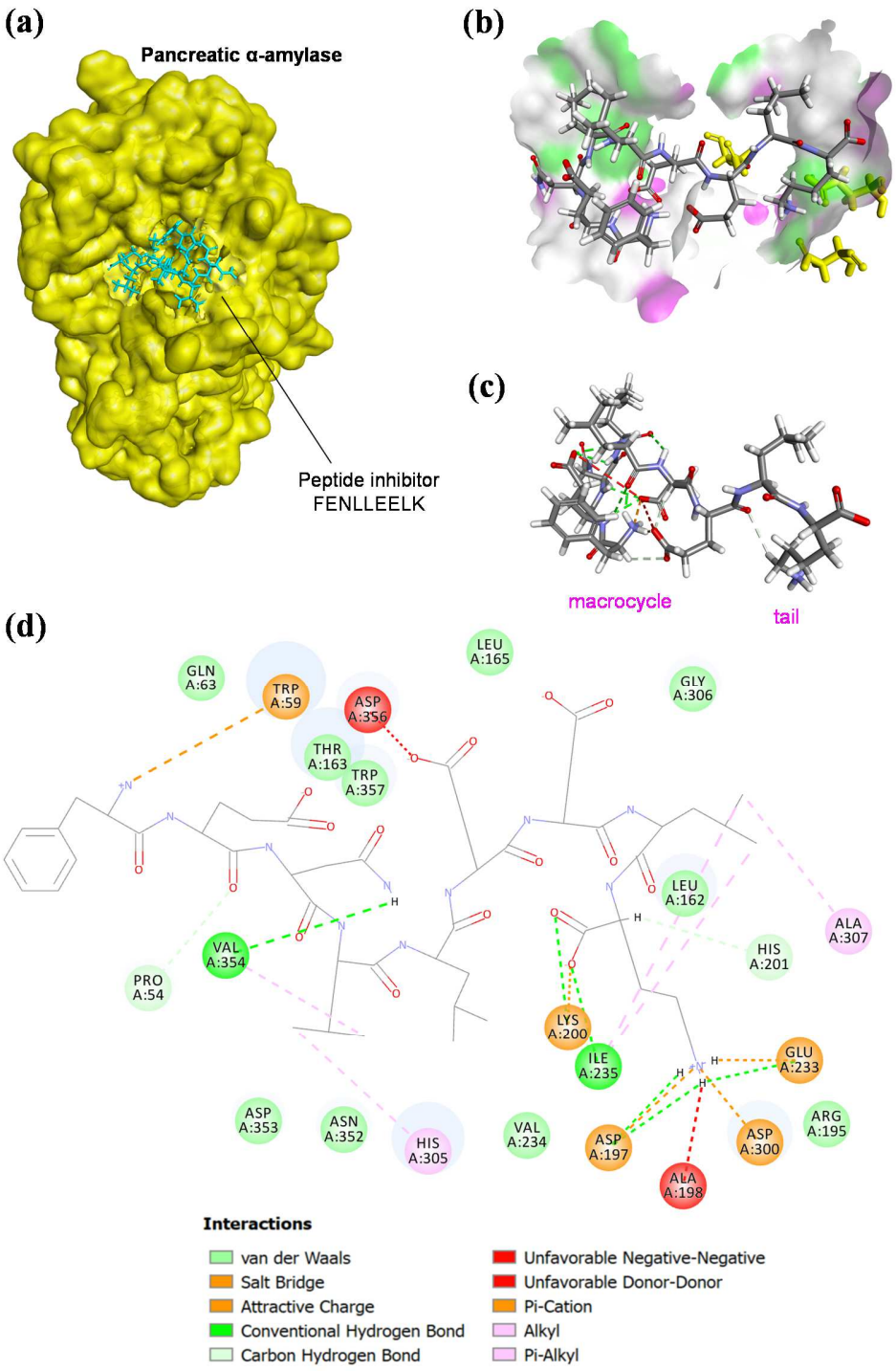
(a)
Pancreatic α-amylase
Peptide inhibitor
FENLLEELK
(b)
(c)
macrocycle
tail
(d)
GLN A:63
TRP A:59
ASP A:356
LEU A:165
GLY A:306
THR A:163
TRP A:357
LEU A:162
ALA A:307
HIS A:201
VAL A:354
PRO A:54
LYS A:200
ILE A:235
GLU A:233
ASP A:353
ASN A:352
HIS A:305
VAL A:234
ASP A:197
ASP A:300
ARG A:195
ALA A:198
Interactions
van der Waals
Salt Bridge
Attractive Charge
Conventional Hydrogen Bond
Carbon Hydrogen Bond
Unfavorable Negative-Negative
Unfavorable Donor-Donor
Pi-Cation
Alkyl
Pi-Alkyl

Fig. 4

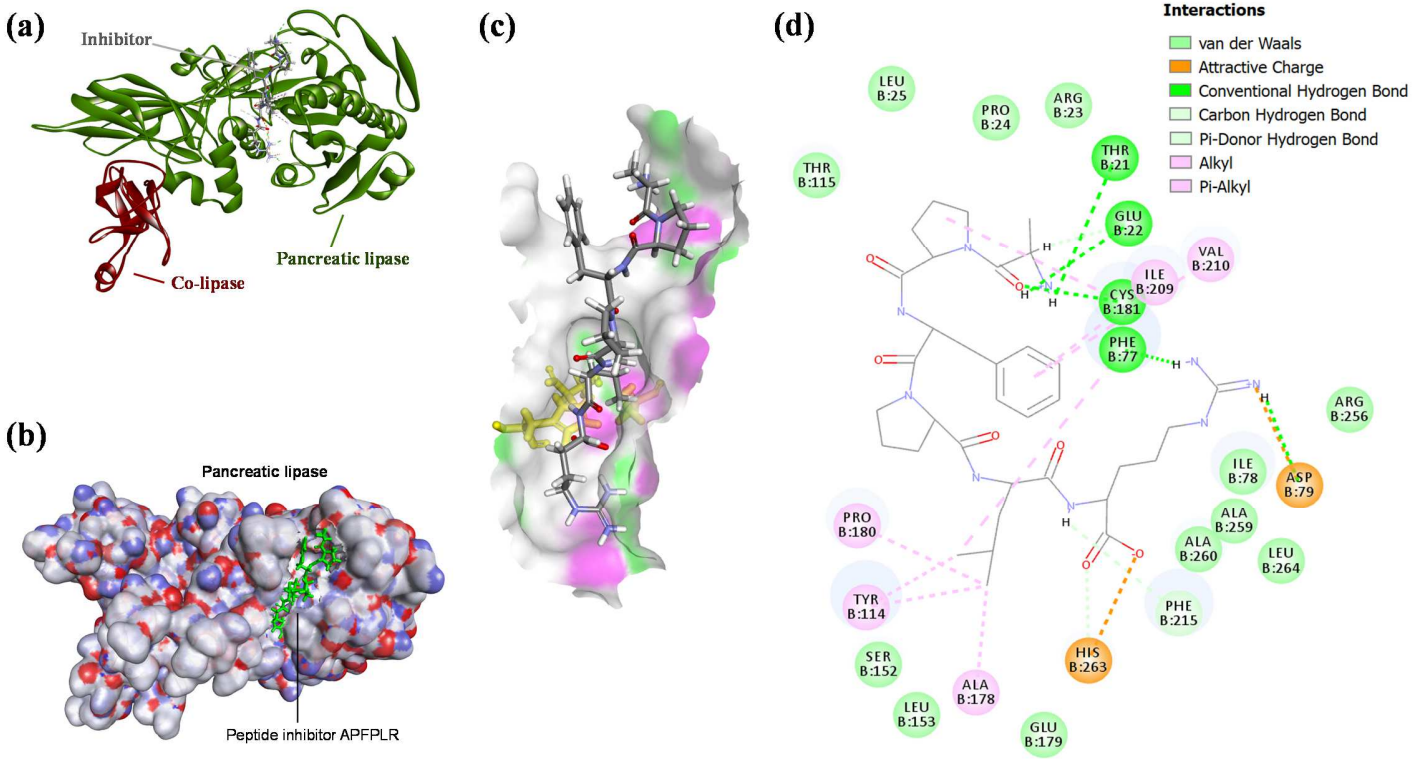
(a)
Inhibitor
Pancreatic lipase
Co-lipase
(b)
Pancreatic lipase
Peptide inhibitor APFPLR
(c)
(d)
Interactions
van der Waals
Attractive Charge
Conventional Hydrogen Bond
Carbon Hydrogen Bond
Pi-Donor Hydrogen Bond
Alkyl
Pi-Alkyl
LEU B:25
PRO B:24
ARG B:23
THR B:115
THR B:21
GLU B:22
VAL B:210
ILE B:209
CYS B:181
PHE B:77
ARG B:256
ILE B:78
ASP B:79
PRO B:180
ALA B:259
ALA B:260
LEU B:264
TYR B:114
PHE B:215
HIS B:263
SER B:152
ALA B:178
LEU B:153
GLU B:179